International Journal of Nanomedicine

Dovepress

open access to scientific and medical research

Open Access Full Text Article

ORIGINAL RESEARCH

# Co-encapsulation of magnetic $Fe_3O_4$ nanoparticles and doxorubicin into biodegradable PLGA nanocarriers for intratumoral drug delivery

This article was published in the following Dove Press journal:
International Journal of Nanomedicine
28 March 2012
Number of times this article has been viewed

Yanhui Jia[1]
Mei Yuan[1]
Huidong Yuan[1]
Xinglu Huang[2]
Xiang Sui[1]
Xuemei Cui[1]
Fangqiong Tang[2]
Jiang Peng[1]
Jiying Chen[1]
Shibi Lu[1]
Wenjing Xu[1]
Li Zhang[1]
Quanyi Guo[1]

[1]Institute of Orthopedics, General Hospital of the Chinese People's Liberation Army, Beijing, People's Republic of China; [2]Laboratory of Controllable Preparation and Application of Nanomaterials, Technical Institute of Physics and Chemistry, Chinese Academy of Sciences, Beijing, People's Republic of China

**Abstract:** In this study, the authors constructed a novel PLGA [poly(D,L-lactic-co-glycolic acid)]-based polymeric nanocarrier co-encapsulated with doxorubicin (DOX) and magnetic $Fe_3O_4$ nanoparticles (MNPs) using a single emulsion evaporation method. The DOX-MNPs showed high entrapment efficiency, and they supported a sustained and steady release of DOX. Moreover, the drug release was pH sensitive, with a faster release rate in an acidic environment than in a neutral environment. In vitro, the DOX-MNPs were easily internalized into murine Lewis lung carcinoma cells and they induced apoptosis. In vivo, the DOX-MNPs showed higher antitumor activity than free DOX solution. Furthermore, the antitumor activity of the DOX-MNPs was higher with than without an external magnetic field; they were also associated with smaller tumor volume and a lower metastases incidence rate. This work may provide a new modality for developing an effective drug delivery system.

**Keywords:** antitumor activity, external magnetic field, intratumoral injection, apoptosis, Lewis lung carcinoma

## Introduction

Doxorubicin (DOX) is an anthracycline glycoside antibiotic originally produced by *Streptomyces peucetius var. caesius*.[1] DOX exerts its cytotoxic effect as a DNA-intercalating agent to inhibit further DNA and RNA biosynthesis.[2] Thus, DOX is widely used either as a single agent or in combination with other chemotherapeutic regimens for various kinds of solid tumors.[3,4] However, dose-limiting toxic side effects such as cardiotoxicity, myelosuppression, mucositis, and alopecia limit the clinical application of DOX, owing to nonspecific distribution to healthy normal tissues.[5] As a result, studies over the past few decades have focused on the development of drug delivery systems and administration routes for DOX to increase tissue selectivity and improve its toxicity profile.[6–8]

Intratumoral administration of chemotherapeutic agents is a potentially more effective modality to overcome the described limitation and this has been extensively evaluated using a number of anticancer drugs.[9,10] Such targeted delivery may realize drug localization within the tumor tissue and divert the drug from nontarget organs to improve toxicity and increase efficacy, while decreasing the incidence and the intensity of side effects.

Although intratumoral administration is a promising approach for the treatment of various solid tumors with minimal systemic toxicity, its efficacy is highly dependent on the timing and frequency of the drug injections because of its rapid clearance from the tumor site. It is proposed that a drug delivery system is required to

Correspondence: Quanyi Guo
Institute of Orthopedics, General Hospital of the Chinese People's Liberation Army, No 28 Fuxing Road, Beijing 100853, People's Republic of China
Tel +86 10 6693 6637
Fax +86 10 6693 9205
Email guoquanyi301@yahoo.com.cn

submit your manuscript | www.dovepress.com
Dovepress
http://dx.doi.org/10.2147/IJN.S28629

ensure the drug is properly localized and that it is released in a controlled way.[11] Several polymeric drug delivery systems have been developed for intratumoral drug delivery, including hydrogels,[9] microparticles,[10] nanoparticles,[12] and nanofibers.[13]

Magnetic nanoparticles (MNPs) have been investigated for decades in drug delivery systems because of their high magnetic responsiveness, biodegradability, biocompatibility, high delivery efficiency and potential targeting function.[14–16] Moreover, iron oxide nanoparticles are the only MNPs approved for clinical use by the US Food and Drug Administration.[17] However, most of the MNP drug delivery systems were developed for systemic administration, which caused severe side effects and inevitable uptake by the reticuloendothelial system (RES).[18] In the present study, the authors propose that combining intratumoral administration with a MNP drug delivery system may provide opportunities for treating cancers in a safe and effective manner. The drug-loaded MNPs are directly injected into solid tumors; they are expected to be held in place by an external magnetic field and to release the drug in a controlled manner.

The authors aimed to develop a MNP drug delivery system for intratumoral administration. A single emulsion evaporation method with magnetic $Fe_3O_4$ cores and a shell of biocompatible polymeric PLGA [poly(D,L-lactic-co-glycolic acid)] was used to prepare the MNPs. The physicochemical properties of the DOX-loaded MNPs (DOX-MNPs) were characterized in terms of morphology, size distribution, and drug loading content. In vitro release profiles of DOX from DOX-MNPs were examined in both acidic and neutral environments. The in vitro anticancer activity of DOX-MNPs was determined using a Lewis lung carcinoma (LLC) cell line, and the apoptotic rate was analyzed by flow cytometry. The uptake of nanoparticles by the LLC cells was visualized using confocal microscopy. Finally, in vivo antitumor activity was assessed by a single intratumoral injection of DOX-MNPs into C57BL/6 mice bearing subcutaneously established LLC.

# Material and methods

## Cell line and cell culture

The murine LLC cells were a gift from Dr Kangla Zong in the Stanford University Medical Center (Stanford, CA). The human osteosarcoma OS-732 cells were purchased from the Beijing Jishuitan Hospital (Beijing, People's Republic of China). The murine-leukemic monocyte-macrophage cell line (RAW 264.7) was purchased from the American Type Culture Collection (Manassas, VA). The cell culture medium and the fetal bovine serum were obtained from Invitrogen (Carlsbad, CA). The culture flasks and dishes were from Corning (New York, NY). The cells were cultured in Dulbecco's modified Eagle medium (DMEM) supplemented with 10% heat-inactivated fetal bovine serum (Invitrogen), penicillin (100 U/mL) (Invitrogen), and streptomycin (100 U/mL) (Invitrogen), and the medium was replaced twice a week. The cultures were maintained at 37°C in a humidified atmosphere containing 5% carbon dioxide.

## Synthesis of $Fe_3O_4$ nanoparticles

The synthesis of aqueous $Fe_3O_4$ nanoparticles was based on coprecipitation of Fe (II) and Fe (III) salts by ammonium hydroxide ($NH_4OH$) at 60°C. In a typical procedure to obtain $Fe_3O_4$ precipitate (1 g), $FeCl_2 \cdot 4H_2O$ (0.86 g) and $FeCl_3 \cdot 6H_2O$ (2.35 g) were dissolved in deionized water (40 mL) with vigorous stirring, such that $Fe^{3+}/Fe^{2+} = 2$. When the solution was heated to 80°C, vigorous stirring was continued for another 30 minutes under a stream of nitrogen, then a solution of oleic acid (100 mg) in acetone (5 mL) was added to the flask, followed by 5 mL of ammonia solution (25% $NH_4OH$) introduced by syringe. After 10 minutes, oleic acid (1 g) was added drop-wise to the suspension and with constant stirring over a 30-minute period. After being heated for an additional 30 minutes, the magnetic particles were precipitated by drop-wise addition of a 2 M hydrochloric acid solution and then washed five times with acetone to remove the excess oleic acid. A total of 30 mL of the ammonia solution (18% $NH_4OH$) and 1 g of oleic acid were added to disperse the magnetic precipitates. The solution had nitrogen bubbled through it and was heated to 80°C for 30 minutes. Finally, the magnetic fluids were stored in an atmosphere of nitrogen.

## Preparation of DOX-MNPs

MNPs containing oleic acid-coated $Fe_3O_4$ nanoparticles and DOX hydrochloride (Taizhou, Zhejiang Hisun Pharmaceutical Co, Ltd, China) were prepared by the conventional oil-in-water single emulsion evaporation method. Three equivalents of triethylamine were added to an aqueous solution of DOX hydrochloride (5 mg/mL), and the drug was then extracted to prepare a methylene chloride solution of DOX. Initially, synthesized nanoparticles were dispersed in methylene chloride, and the resulting dispersion was mixed with the methylene chloride solution of DOX. PLGA (20 mg) was added to the solution of oleic

acid-coated $Fe_3O_4$ nanoparticles and DOX (1 mL). This mixture was emulsified in aqueous solution (100 mL) of Pluronic F-127 (7 wt %) by use of a probe-type sonicator at 600 W for 10 minutes in an ice bath. The resulting suspension was stirred for 12 hours at room temperature to evaporate the organic solvent and was then centrifuged at 10,000 rpm for 10 minutes. The precipitate was washed twice in water to remove the remaining Pluronic F-127 and free PLGA. The supernatant was used for the analysis of DOX loading efficiency.

For evaluation of drug contents and drug loading efficiency, freeze-dried DOX-MNPs (5 mg) were dissolved in dimethyl sulfoxide (10 mL). The DOX concentration was evaluated using an ultraviolet and visible spectrophotometer (UV-1201; Shimadzu, Kyoto, Japan) at 480 nm. Empty nanoparticles of PLGA were used as a blank test.

$$\text{Loading contents} = (\text{Drug weight in the nanoparticles} / \text{Weight of nanoparticles}) \times 100\% \quad (1)$$

$$\text{Encapsulation efficiency} = (\text{Residual drug in the nanoparticle} / \text{Initial feeding amount of drug}) \times 100\% \quad (2)$$

## Physicochemical properties of DOX-MNPs

The size and morphologic features of DOX-MNPs were examined using dynamic light scattering and transmission electron microscopy. DOX-MNPs were diluted to a concentration of 1 mg/mL with deionized water. The DOX-MNPs were stained with 1% uranyl acetate and examined with a JEOL 100 CX electron microscope (JEOL USA, Inc, Peabody, MA). DOX-MNP size was determined with a Zetasizer 5000 (Malvern Instruments Ltd, Malvern, UK).

To determine the kinetics of in vitro release of DOX from DOX-MNPs, freeze-dried DOX-MNPs (1 mg) were transferred to a dialysis tube (MEMBRA-CEL®, MW cutoff, 12000; Viskase Companies, Inc, Darien, IL), and the sealed tube was introduced into a vial containing 10 mL of either phosphate buffered saline (PBS) (pH 7.4) or acetate buffer (pH 5.0). The vials were shaken horizontally in a shaking water bath (100 rpm) at 37°C for 168 hours. At predetermined time intervals, 2 mL samples of the medium were collected and replaced with the same amount of fresh medium. The amount of released DOX was analyzed by measuring the absorbance of the sample at 488 nm with the ultraviolet and visible spectrophotometer.

## Cellular uptake of DOX-MNPs

LLC, OS-732, and RAW 264.7 cells were plated on 14 $mm^2$ glass coverslips that were placed in six-well plates at the density of $5 \times 10^5$ cells/well; to allow cell attachment, these were cultured at 37°C for 24 hours in an atmosphere containing 5% carbon dioxide. DOX-MNPs or free DOX were diluted with culture medium to 5 μg/mL, followed by coculture with aforementioned cell lines for 30, 60, and 120 minutes. The uptake experiment was terminated at each time point by aspirating the test samples and washing the cell monolayers with ice-cold PBS three times. Each cell monolayer on the coverslips was then fixed with methanol-acetone (1:1, v/v), followed by nuclear staining with Hoechst 33258 and examination under fluorescence microscopy. The uptake of DOX-MNPs or free DOX can be visualized by virtue of the intrinsic red fluorescence of DOX. Fluorescence intensity was analyzed on a fluorescence microscope (Eclipse E800; Nikon, Tokyo, Japan) at a wavelength of 488 nm.

## Analysis of apoptosis using Annexin V and propidium iodide staining by flow cytometry

Apoptotic cells were identified with fluorescein isothiocyanate-labeled Annexin V (Annexin V-FITC). Propidium iodide (PI) (BioVision, Mountain View, CA), a dead cell marker, was also used as a stain, and according to the manufacturer's protocol. LLC cells were plated at $5 \times 10^5$ cells per well in DMEM (2 mL) in six-well plates and grown for 24 hours. The medium was then replaced with a series of concentrations of DOX-MNPs (1, 5, and 10 μg/mL) for 48 hours. All drugs were diluted with DMEM, and cells treated with DMEM alone were used as a control. Briefly, treated cells were harvested, trypsinized, washed with PBS, incubated with Annexin V-FITC and PI for 15 minutes at room temperature in the dark, and analyzed on a FACSCalibur flow cytometer (Becton, Dickinson and Company, Mountain View, CA) with data acquisition software (CellQuest; Becton, Dickinson and Company).

## In vivo antitumor activity in a murine model

Female C57BL/6 mice (6 weeks old) were obtained from the Institute of Materia Medica, Chinese Military Academy of Medical Sciences (Beijing, People's Republic of China). All animal procedures in this study followed the protocol approved by the Institutional Animal Care and Use Committee of the Chinese Academy of Sciences.

Murine LLC cells (about $5 \times 10^5$ cells per 0.2 mL) were implanted subcutaneously into the backs of the mice. When the tumor volumes reached $5 \times 5 \times 4$ mm, 60 tumor-bearing mice were randomly assigned to one of the following six treatment groups (n = 10 per group): (1) DOX-MNPs (10 mg/kg, single dose) with an external magnetic field; (2) DOX-MNPs only (10 mg/kg, single dose); (3) MNPs (107.6 mg/kg, single dose) with an external magnetic field; (4) MNPs alone (107.6 mg/kg, single dose); (5) free DOX solution (10 mg/kg, single dose); and (6) control (0.9% sodium chloride). All drugs were diluted with 0.9% sodium chloride (100 μL), and all were administered through direct intratumoral injection. After drug administration, mortality was monitored daily and tumor growth was determined by caliper measurement at 3-day intervals over 14 days. Tumor volume was calculated as follows:

$$\text{Tumor volume } (mm^3) = (\text{Length} \times \text{Width}^2)/2 \quad (3)$$

For the treatment groups with an external magnetic field, a disk magnet with a magnetic field strength of 0.5 tesla (neodymium iron boron, 10 mm diameter, 2 mm thickness) was fixed onto the skin above the tumor immediately after the drug was injected into the tumor, and the magnet was held in place for 48 hours.

## Histological examination

After the mice were sacrificed, the tumors, hearts, livers, spleens, lungs, and kidneys were immediately harvested, weighed, fixed in 10% formalin, and embedded in paraffin. Sections were observed by light microscopy after they had been stained with hematoxylin and eosin and Perls' Prussian blue.

## Statistical analysis

All data were analyzed with SPSS software (v 13.0; SPSS Inc, Chicago, IL). Results are presented as mean plus or minus standard deviation. The two-way analysis of variance and Student's *t*-test were used to compare data from different treatment groups, and differences were considered significant at $P < 0.05$.

# Results

## Physicochemical properties of DOX-MNPs

The DOX-MNPs containing magnetic $Fe_3O_4$ cores and DOX were prepared using an oil-in-water emulsion and a subsequent solvent evaporation method. The morphologic features observed by transmission electron microscopy showed that the size distribution (in diameter) of the MNPs was between 4 and 6 nm (Figure 1A) and the size distribution of DOX-MNPs was generally between 200 and 300 nm (Figure 1B). The Zetasizer showed a narrow particle size distribution, with an average diameter of about 280 nm (Figure 1C). The DOX-MNPs showed excellent magnetic responsiveness and dispersibility in aqueous solution: they were easily dispersed in water and could be drawn from the aqueous solution by a permanent magnet (Figure 1D).

## Encapsulation efficiency

Encapsulation efficiency was defined as the weight percentage of DOX incorporated into DOX-MNPs. When the weight ratio of DOX to PLGA was 20 μg/mg, the encapsulation efficiency was approximately 90%. The loading content was 85 μg/mg.

## Drug release profile in vitro

The in vitro release of DOX from the DOX-MNPs showed a sustained release pattern under neutral (pH 7.4) and acidic (pH 5.0) conditions. The drug release from DOX-MNPs was much slower at pH 7.4 than at pH 5.0. After 7 days of incubation, approximately 65% of the total drug was released in pH 5.0 conditions, in comparison with a 25% release rate in pH 7.4 conditions (Figure 2).

## Cellular uptake of DOX-MNPs

DOX-MNPs were added to LLC, OS-732, and RAW 264.7 cells, and were then incubated separately for 30, 60, and 120 minutes. The cells were collected for analysis of intrinsic fluorescence of DOX by fluorescence microscopy. LLC (Figure 3A), OS-732 (Figure 3B), and RAW 264.7 cells (Figure 3B) internalized DOX-MNPs at each time point.

## DOX-MNPs-induced apoptosis of tumor cells

The percentage of apoptotic and necrotic cells was quantified by Annexin V-FITC and PI assay in LLC cells. The LLC cells were treated with fresh medium containing three different concentrations of DOX-MNPs (1 μg/mL, 5 μg/mL, and 10 μg/mL). The dead cells increased in proportion to dosage (Figure 4A and B). To compare the apoptosis activity of DOX-MNPs and free DOX on tumor cells, LLC cells were exposed to free DOX (5 μg/mL) or equivalent

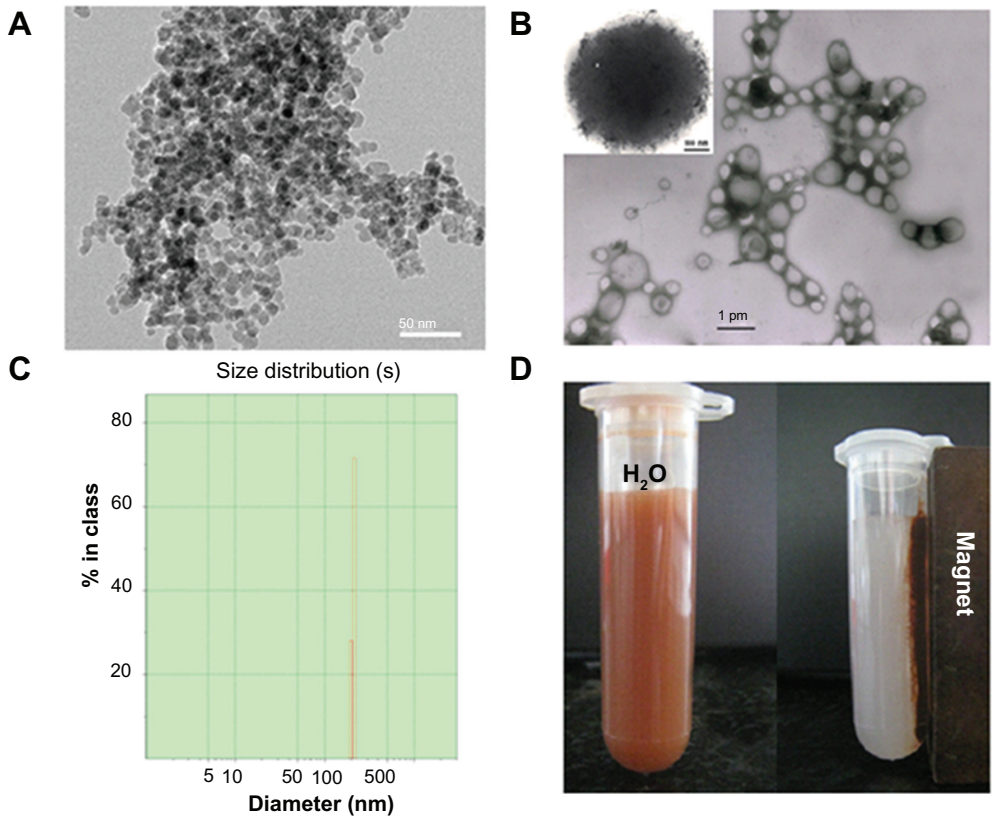


**Figure 1** Physicochemical characterization of doxorubicin-loaded magnetic $Fe_3O_4$ nanoparticles (DOX-MNPs): (**A**) transmission electron microscopy images of oleic acid-coated MNPs; (**B**) transmission electron microscopy images of DOX-MNPs; (**C**) size distribution of DOX-MNPs; (**D**) DOX-MNPs dispersed in aqueous solution could be attracted by an external magnetic field.

concentrations of DOX-MNPs for 48 hours. The percentage of dead cells in the DOX-MNPs (80%) was higher than in the free DOX (29%), whereas the percentage of necrotic cells in untreated and MNP-treated cells was less than 20% (Figure 4C and D).

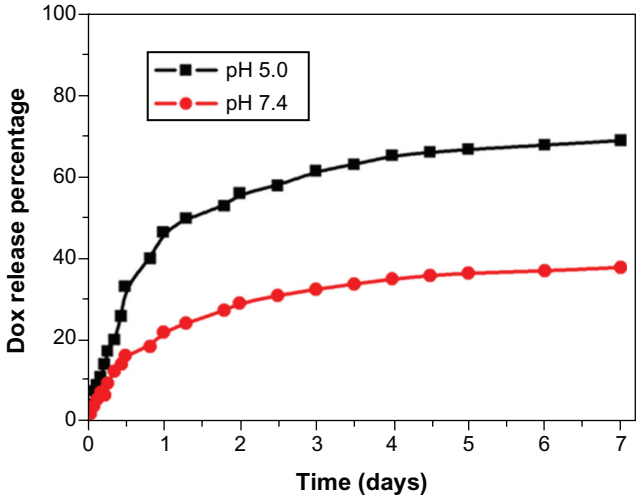


**Figure 2** In vitro release profile of doxorubicin (DOX) from DOX-loaded magnetic $Fe_3O_4$ nanoparticles at pH 5.0 in acetate buffer and pH 7.4 in phosphate buffered saline.
**Note:** The results presented show the average from three measurements.

## Antitumor effect of DOX-MNPs in vivo

The authors compared the antitumor effect of DOX-MNPs with or without an external magnetic field and free DOX in the subcutaneous tumor model of LLC. On day 14, the average tumor size in the saline control group was 2.311 $cm^3$, in the group receiving free DOX alone it was 1.911 $cm^3$, in the group receiving DOX-MNPs it was 1.498 $cm^3$, and in the group receiving DOX-MNPs with an external magnetic field it was 1.027 $cm^3$. The sizes with MNPs alone and MNPs with external magnetic field treatment were 2.212 and 2.295 $cm^3$, respectively. The tumor size in mice receiving DOX-MNPs with an external magnetic field was significantly smaller than in the control mice ($P = 0.027$). The tumor growth curve is shown in Figure 5. Tumor growth rates in mice treated with DOX-MNPs and an external magnetic field were significantly decreased, whereas free DOX treatment only slightly reduced the tumor growth.

There was no weight loss observed in the mice, including the mice treated with DOX-MNPs and an external magnetic field.

There were no lesions in the main organs, including the heart, liver, lungs, pancreas, and kidneys. Tumor metastasis

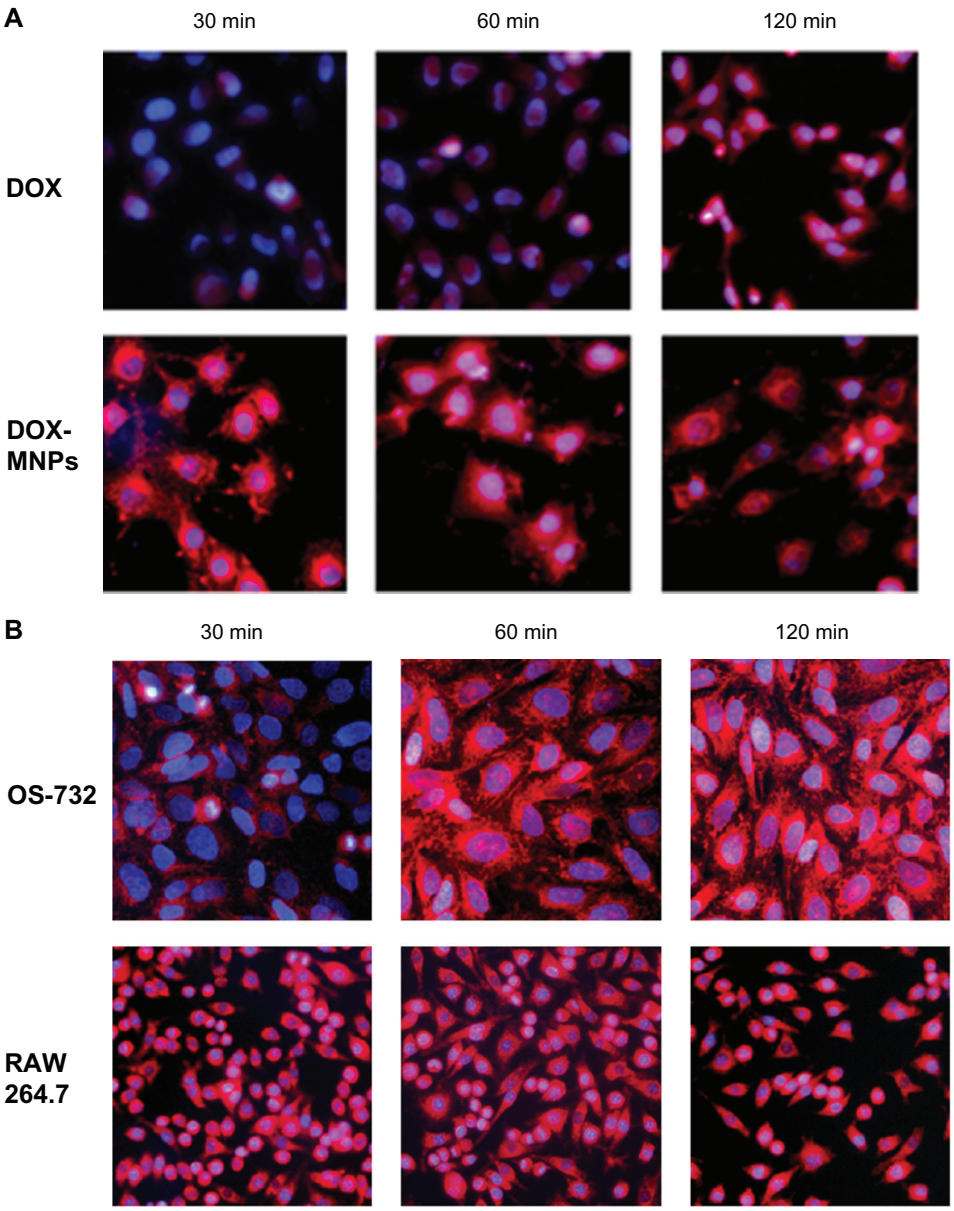


**Figure 3** Observation of cellular uptake of doxorubicin-loaded magnetic $Fe_3O_4$ nanoparticles (DOX-MNPs) by different cell types after 30, 60, and 120 minutes of incubation under a fluorescence microscope. Overlaid images show nuclear staining with Hoechst 33258 (blue) and DOX-derived fluorescence (red). (**A**) Cellular uptake of free DOX and DOX-MNPs by Lewis lung carcinoma cells; (**B**) cellular uptake of DOX-MNPs by human osteosarcoma OS-732 cells and RAW 264.7 cells (murine-leukemic monocyte-macrophage cell line).

was found in the lungs, kidneys, and, occasionally, liver and heart. The incidence of metastasis was highest in the control group and lowest in the group receiving DOX-MNPs with an external magnetic field (Table 1).

The penetration of tumors and organs by the MNPs was analyzed by hematoxylin and eosin and Perls' Prussian blue staining. The blue-stained cells were found in tumor cells in groups receiving $Fe_3O_4$ treatment (Figure 6A and B), and in some lung metastasis tumor cells (Figure 6C), but not in the saline control or free DOX-treated tumor cells. The $Fe_3O_4$-positive tumor cells were more abundant in the groups treated with an external magnetic field than those treated with MNPs only (Figure 6A and B). In the groups treated with MNPs, $Fe_3O_4$ was deposited in the kidney tubule in a couple of cases (one in the DOX-MNP group and one in the MNP group) and, (although only occasionally) under the capsule of the spleen in one case (in the MNP group). However, no $Fe_3O_4$ was deposited in the groups treated with an external magnetic field.

## Discussion

The intratumoral administration of anticancer drugs represents a growing trend for maximizing local tumor control with

minimal systemic toxicity; however, it requires a novel drug delivery system for treatment efficacy and ease of administration. MNPs have been widely used in the delivery of chemotherapeutics, achieving promising results.[19–23] The authors propose that combining intratumoral administration with a magnetic nanocarrier in chemotherapy provides opportunities for treating cancers in a safe and effective manner. In this study, the authors fabricated a MNP drug delivery system for intratumoral administration that was comprised of magnetic $Fe_3O_4$ cores and a shell of biocompatible polymeric PLGA by a single emulsion evaporation method. The DOX-MNPs showed high loading content and encapsulation

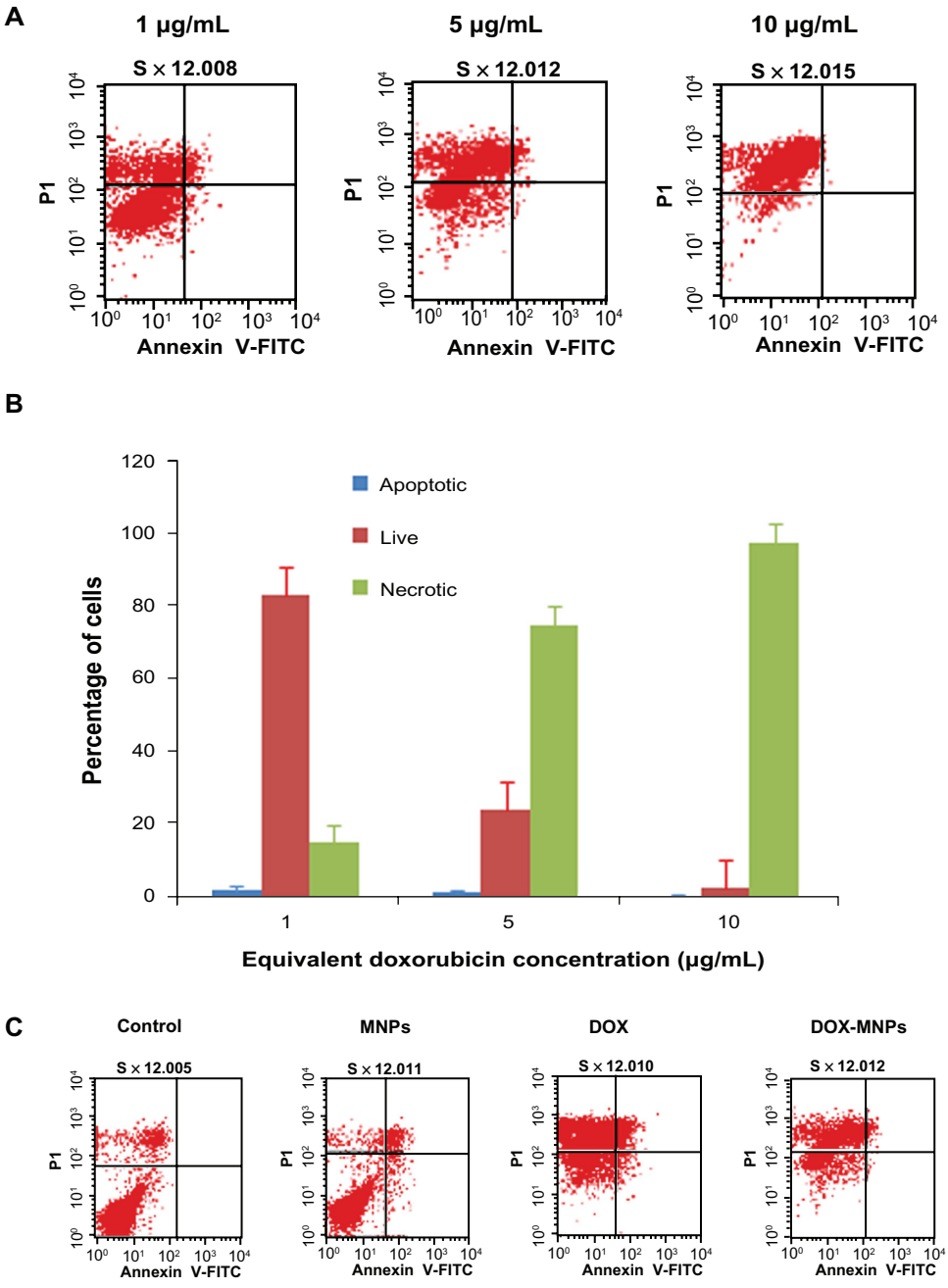


**Figure 4** The apoptosis-induction effect of doxorubicin-loaded magnetic $Fe_3O_4$ nanoparticles (DOX-MNPs) in Lewis lung carcinoma cells (LLC). Fluorescein isothiocyanate–labeled Annexin V (Annexin V-FITC) and propidium (PI) double staining and flow cytometry were used to determine the proportion of live cells (Annexin V-FITC and PI double negative, bottom left quadrant), early apoptotic cells (Annexin V-FITC and PI negative, bottom right quadrant), late apoptotic cells (Annexin V-FITC and PI positive, top left quadrant), and necrotic cells (Annexin V-FITC and PI double positive, top right quadrant). (**A**) Representative histograms from flow cytometry of LLC cells treated with medium containing a series of concentrations of DOX-MNPs; (**B**) determination of live, apoptotic, and necrotic cells treated with a series of concentrations of DOX-MNPs; (**C**) representative histograms from flow cytometry of LLC cells treated with fresh medium containing free DOX (5 μg/mL) or equivalent concentrations of MNPs and DOX-MNPs; (**D**) determination of live, apoptotic and necrotic cells treated with free DOX (5 μg/mL) or equivalent concentrations of MNPs and DOX-MNPs.

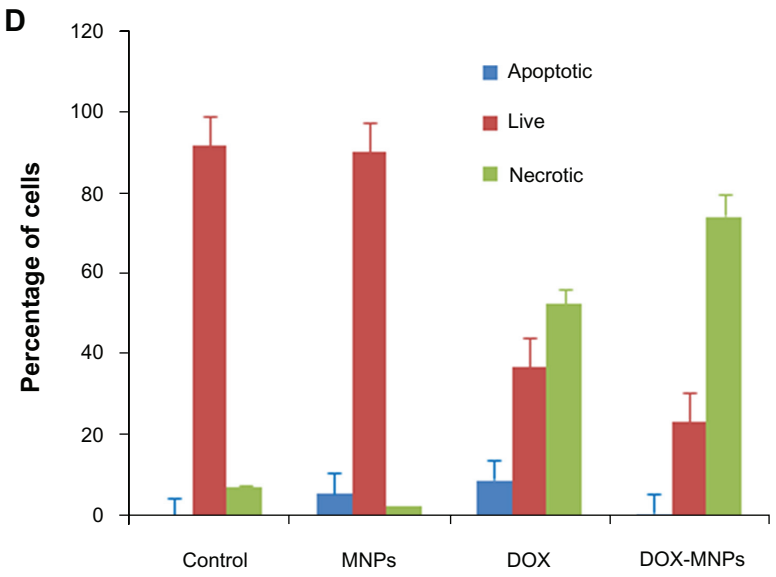


**Figure 4** (*Continued*)

efficiency, and they supported a sustained and steady release of DOX. In vitro, the DOX-MNPs were easily internalized into tumor cells and they induced apoptosis. In vivo, the DOX-MNPs showed higher antitumor activity than the free DOX solution.

Systemic chemotherapy against cancers such as breast, prostate, lung, and gastrointestinal cancers can cause severe side effects because of the toxicity of the anticancer drugs on normal tissues. Moreover, the efficacy of anticancer drugs can be diminished because of rapid clearance from the circulation and poor distribution to the target tumor.[24,25] Intravenously injected free DOX was exposed to rapid elimination by the RES, mainly in the liver and spleen.[26] Even long-circulating formulations of free DOX were not capable of achieving tumor exposure to DOX for more than 180 hours.[27] An intratumoral injection of chemotherapeutic agents is potentially a more effective alternative to systemic administration, because direct delivery of the anticancer drug to the target may improve both the stability and the efficacy of anticancer drugs.[28] Such targeted delivery would be expected to provide a high local concentration of agents, reducing systemic drug levels and thereby decreasing the incidence of side effects compared with traditional treatments.

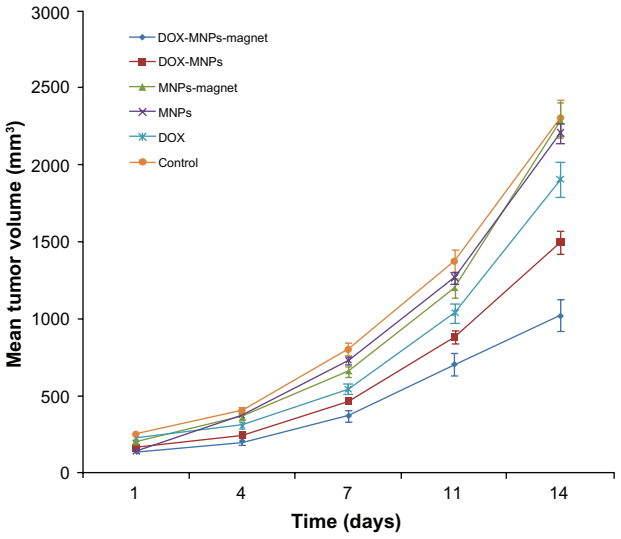


**Figure 5** Antitumor effect of doxorubicin-loaded magnetic $Fe_3O_4$ nanoparticles (DOX-MNPs) in mice bearing subcutaneously established Lewis lung carcinoma.
**Note:** Tumor volume data given as mean plus or minus standard deviation.

The size of the nanoparticles is a key parameter that determines its properties, application and fate. First, given that the smallest capillaries in the body are about 4 μm, particles larger than 4 μm will most likely become trapped in the lungs.[17] Particles smaller than that will usually be eliminated by the mononuclear phagocytes system, a part of the body's immune system also known as the RES. These involve the family of cells (primarily monocytes and macrophages) that are extensively distributed in the liver (Kupffer cells), spleen, bone marrow, and lymph nodes. Because of the greater accessibility, the macrophages in the liver and spleen will take up most of the particles. After intravenous administration, particles larger than 200 nm are usually sequestered by the spleen, as a result of mechanical filtration.[29] These particles are eventually removed by the cells of the phagocyte system,[29] resulting in decreased blood circulation times. On the other hand, particles smaller than 10 nm are rapidly removed through extravasations and

**Table 1** Metastasis of Lewis lung carcinoma in mice after treatment

| Treatment | Mice (n) | Lung | | | Kidney | | Liver | Heart | Total metastasis rate |
|---|---|---|---|---|---|---|---|---|---|
| | | Large | Medium | Small | Large | Small | Small | Medium | |
| Dox-MNPs-magnet | 8 | 2 | 0 | 1 | 1 | 0 | 0 | 0 | 50.0% (4/8) |
| Dox-MNPs | 10 | 2 | 2 | 2 | 1 | 0 | 1 | 0 | 60.0% (6/10) |
| MNPs-magnet | 6 | 1 | 1 | 2 | 1 | 0 | 0 | 0 | 66.7% (4/6) |
| MNPs | 7 | 3 | 2 | 1 | 2 | 0 | 0 | 0 | 85.7% (6/7) |
| DOX | 9 | 2 | 1 | 1 | 3 | 1 | 0 | 1 | 66.7% (6/9) |
| Control | 8* | 4 | 2 | 1 | 1 | 0 | 0 | 0 | 87.5% (7/8) |

**Note:** *Some mice specimens were not included because the autopsy had not been performed immediately after the mouse was sacrificed.
**Abbreviations:** DOX, doxorubicin; magnet, external magnetic field; MNPs, magnetic $Fe_3O_4$ nanoparticles.

renal clearance.[29,30] Particles ranging from 10 to 100 nm are optimal for systemic administration and demonstrate the most prolonged blood circulation times.[31] The particles in this size range are small enough to both evade the RES and penetrate the very small capillaries within the body tissues, and therefore they may offer the most effective distribution in certain tissues. Attempts have been made to retard the action of the RES and increase the half-life in the blood stream, such as by reducing the particle size and surface modification.[32] However, despite all efforts, complete evasion of the RES does not seem feasible, and unwanted migration to normal tissues in the body could cause toxic side effects.

One advantage of drug delivery systems using MNPs is the controlled drug release, which improves the drug

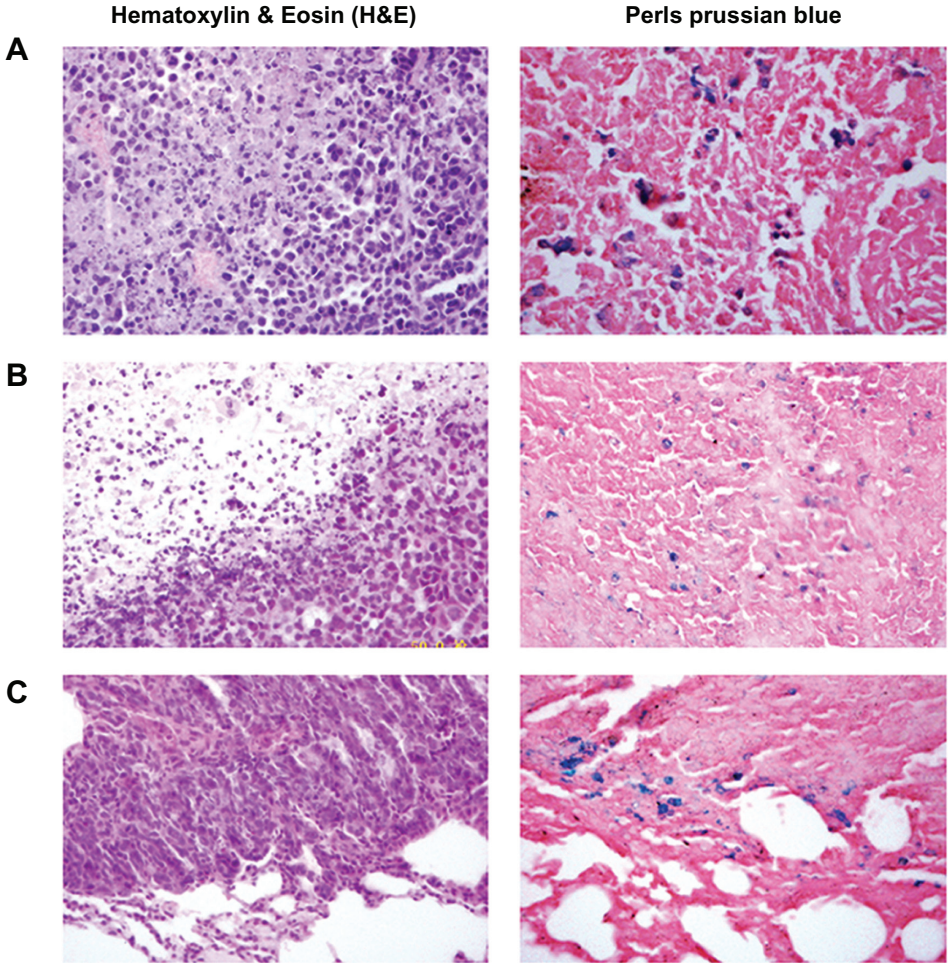


**Figure 6** Histological analysis of the uptake of doxorubicin-loaded magnetic $Fe_3O_4$ nanoparticles (DOX-MNPs) in tumors (blue indicated the presence of iron): (**A**) marked accumulation of DOX-MNPs was observed in tumor cells with an external magnetic field; (**B**) less accumulation of DOX-MNPs in tumor cells without an external magnetic field; (**C**) accumulation of DOX-MNPs in lung metastasis of Lewis lung carcinoma.

bioavailability and reduces the side effects and toxicity to healthy tissues. Because of its excellent biocompatibility and biodegradability, PLGA has been widely employed as a matrix material for preparation of nanoparticles for drug, gene, or imaging agent delivery. Changing the comonomer composition and molecular weight of PLGA can control the drug release rate from PLGA nanoparticles.[33] Since the acidic pH is now regarded as a phenotype of the growth and invasiveness of solid tumors,[34,35] developing pH-sensitive delivery systems seems to be a promising approach for chemotherapy. In the present study, the DOX release rate from PLGA nanoparticles was higher at the acidic pH (pH 5.0) than at the neutral pH (pH 7.4), which may lead to increased accumulation of DOX in tumor cells and thereby adding therapeutic efficiency to the delivery system.

After delivery to the tumor site, the next important step is internalization into the tumor cell. This is directly related to the cytotoxicity of the drug, because the most commonly used chemotherapeutic drugs such as DOX and paclitaxel only show their antitumor efficiency when they bind to DNA or inhibit microtubule disassembly.[36] In this study, the authors found the DOX-MNPs was readily taken up by LLC, OS-732, and RAW 264.7 cells, with a higher rate of cellular uptake and of larger amount than free DOX. In fact, the nanoparticles allow for efficient uptake by a variety of cell types and selective drug accumulation at target sites.[37,38] Other authors working with MNPs – used in hyperthermia,[39] cancer diagnosis and biodistribution studies,[40] and cancer therapy[41] – have reported such facile cellular uptake. The DOX-MNPs can be transported into tumor cells by a process called endocytosis or phagocytosis, through either specific or nonspecific cellular uptake, depending on the surface properties of the MNPs.[42] However, the exact mechanism of cellular uptake may be far more complicated than the current understanding, and further studies are clearly needed.

In vitro, the DOX-MNPs was found to show a higher apoptosis-inducing effect in the LLC cell line than free DOX. These results are in agreement with previous reports. Kohler et al[43] reported that methotrexate-immobilized poly(ethylene glycol) MNPs induce higher cytotoxicity in glioma cells than free methotrexate, depending on higher uptake and retaining its crystal structure in the cell cytoplasm. Chen et al[44] reported that the application of 5-bromotetrandrine and MNP of $Fe_3O_4$ inhibited the expression of Bcl-2 protein and upregulated the expression of BAX and caspase-3 proteins in human leukemia K562/A02 cells. Jiang et al[45] reported expressions of multidrug resistance proteins MDR1, lung resistance-related protein, and P-glycoprotein were decreased. Therefore, MNPs may suppress tumor cell proliferation and induce apoptosis by blocking multiple pathways.

In vivo, the DOX-MNPs showed higher antitumor efficacy than free DOX on subcutaneous LLC tumor-bearing models. The authors chose to administer only a single dose of DOX (10 mg/kg body weight) or an equivalent dose of DOX-MNPs to the tumor site. The tumor growth rate was not found to significantly decrease with free DOX treatment; however, the tumor growth rate was significantly decreased in the group treated with DOX-MNPs with an external magnetic field, and the rate of metastasis was also decreased. Meanwhile, the concentration of $Fe_3O_4$ particles inside tumor cells was found to increase when a simple external magnetic field was applied, indicating the concentration of DOX in the tumor was increased. These results were similar to previous results that stated only using an external magnetic field was effective. Widder et al[46] demonstrated the utility of magnetic albumin microspheres in animal tumor models. Significantly greater responses, in terms of both tumor size and animal survival, were achieved with magnetic albumin microspheres than with DOX alone. Gupta and Hung[47] demonstrated that the efficacy of magnetic microspheres in the targeted delivery of an incorporated drug is predominantly due to the magnetic effects, not the particle's size or nonmagnetic holding. Smaller tumor volumes were found in the groups treated with DOX-MNPs under a magnetic field than in those receiving treatment without a magnetic field. Reasons for the higher antitumor activity may be higher concentration of DOX-MNPs in the tumor site, facile cellular uptake by tumor cells, and sustained drug release in the microenvironment. In this study, the DOX-MNPs were administered through a direct intratumoral injection to evade the RES; the external magnetic field may hold the nanoparticles in place rather than guiding or targeting the nanoparticles to the tumor site.

## Conclusion

In summary, the authors constructed a PLGA-based polymeric nanocarrier coencapsulated with DOX and MNPs by a single emulsion evaporation method for intratumoral drug delivery. The nanoparticles supported sustained and steady release of DOX. Moreover, the drug release from the DOX-MNPs was pH sensitive, with a faster release rate in an acidic environment than in a neutral environment. In vitro, the DOX-MNPs were readily internalized into tumor cells, and they induced a higher apoptosis rate. In vivo, the DOX-MNPs showed higher rates

of antitumor activity than free DOX solution. Furthermore, applying an external magnetic field enhanced the antitumor activity of the DOX-MNPs, with smaller tumor volumes and lower rates of metastases incidence being exhibited. This work provides an exciting new modality for developing an effective drug delivery system.

## Acknowledgments

The National High Technology Research and Development Program of China (863, No 2007AA021806) supported this work. The authors are thankful to Ms Sylvia Chang at the University of California, Los Angeles, for her assistance in the English editing of the manuscript.

## Disclosure

The authors declare they have no financial or personal relationships with other people or organizations that can inappropriately influence this work, and they have no professional or personal interest of any nature in any product, service, or company that could be construed as influencing the position presented in this work.

## References

1. Hortobágyi GN. Anthracyclines in the treatment of cancer: an overview. *Drugs*. 1997;54 Suppl 4:1–7.
2. Goodman MF, Lee GM. Adriamycin interactions with T4 DNA polymerase: two modes of template-mediated inhibition. *J Biol Chem*. 1977;252(8):2670–2674.
3. Gehl J, Boesgaard M, Paaske T, Vittrup Jensen B, Dombernowsky P. Combined doxorubicin and paclitaxel in advanced breast cancer: effective and cardiotoxic. *Ann Oncol*. 1996;7(7):687–693.
4. Yousefpour P, Atyabi F, Farahani EV, Sakhtianchi R, Dinarvand R. Polyanionic carbohydrate doxorubicin-dextran nanocomplex as a delivery system for anticancer drugs: in vitro analysis and evaluations. *Int J Nanomedicine*. 2011;6:1487–1496.
5. Kang YM, Kim GH, Kim JI, et al. In vivo efficacy of an intratumorally injected in situ-forming doxorubicin/poly(ethylene glycol)-b-polycaprolactone diblock copolymer. *Biomaterials*. 2011;32(20):4556–4564.
6. Gao ZG, Lee DH, Kim DI, Bae YH. Doxorubicin loaded pH-sensitive micelle targeting acidic extracellular pH of human ovarian A2780 tumor in mice. *J Drug Target*. 2005;13(7):391–397.
7. Weinberg BD, Ai H, Blanco E, Anderson JM, Gao J. Antitumor efficacy and local distribution of doxorubicin via intratumoral delivery from polymer millirods. *J Biomed Mater Res A*. 2007;81(1):161–170.
8. Chen Y, Wan Y, Wang Y, Zhang H, Jiao Z. Anticancer efficacy enhancement and attenuation of side effects of doxorubicin with titanium dioxide nanoparticles. *Int J Nanomedicine*. 2011;6:2321–2326.
9. Al-Abd AM, Hong KY, Song SC, Kuh HJ. Pharmacokinetics of doxorubicin after intratumoral injection using a thermosensitive hydrogel in tumor-bearing mice. *J Control Release*. 2010;142(1):101–107.
10. Xie M, Zhou L, Hu T, Yao M. Intratumoral delivery of paclitaxel-loaded poly(lactic-co-glycolic acid) microspheres for Hep-2 laryngeal squamous cell carcinoma xenografts. *Anticancer Drugs*. 2007;18(4): 459–466.
11. Emerich DF, Snodgrass P, Lafreniere D, et al. Sustained release chemotherapeutic microspheres provide superior efficacy over systemic therapy and local bolus infusions. *Pharm Res*. 2002;19(7):1052–1060.
12. Chang GT, Li C, Lu WY, Ding JD. N-Boc-histidine-capped PLGA-PEG-PLGA as a smart polymer for drug delivery sensitive to tumor extracellular pH. *Macromol Biosci*. 2010;10(10):1248–1256.
13. Xu XL, Chen XS, Wang ZF, Jing XB. Ultrafine PEG-PLA fibers loaded with both paclitaxel and doxorubicin hydrochloride and their in vitro cytotoxicity. *Eur J Pharm Biopharm*. 2009;72(1):18–25.
14. Xie J, Huang J, Li X, Sun S, Chen X. Iron oxide nanoparticle platform for biomedical applications. *Curr Med Chem*. 2009;16(10):1278–1294.
15. Chen B, Cheng J, Shen M, et al. Magnetic nanoparticle of $Fe_3O_4$ and 5-bromotetrandrin interact synergistically to induce apoptosis by daunorubicin in leukemia cells. *Int J Nanomedicine*. 2009;4: 65–71.
16. Wang J, Chen Y, Chen B, et al. Pharmacokinetic parameters and tissue distribution of magnetic Fe(3)O(4) nanoparticles in mice. *Int J Nanomedicine*. 2010;5:861–866.
17. Neuberger T, Schopf B, Hofmann H, Hofmann M, von Rechenberg B. Superparamagnetic nanoparticles for biomedical applications: possibilities and limitations of a new drug delivery system. *J Magn Magn Mater*. 2005;293(1):483–496.
18. Arruebo M, Fernández-Pacheco R, Ibarra MR, Santamaría J. Magnetic nanoparticles for drug delivery. *Nano Today*. 2007;2(3):22–32.
19. McBain SC, Yiu HH, Dobson J. Magnetic nanoparticles for gene and drug delivery. *Int J Nanomedicine*. 2008;3(2):169–180.
20. Widder KJ, Morris RM, Poore G, Howard DP Jr, Senyei AE. Tumor remission in Yoshida sarcoma-bearing rats by selective targeting of magnetic albumin microspheres containing doxorubicin. *Proc Natl Acad Sci U S A*. 1981;78(1):579–581.
21. Lübbe AS, Bergemann C, Huhnt W, et al. Preclinical experiences with magnetic drug targeting: tolerance and efficacy. *Cancer Res*. 1996; 56(20):4694–4701.
22. Lübbe AS, Bergemann C, Riess H, et al. Clinical experiences with magnetic drug targeting: a phase I study with 4′-epidoxorubicin in 14 patients with advanced solid tumors. *Cancer Res*. 1996;56(20):4686–4693.
23. Alexiou C, Jurgons R, Schmid RJ, et al. Magnetic drug targeting–biodistribution of the magnetic carrier and the chemotherapeutic agent mitoxantrone after locoregional cancer treatment. *J Drug Target*. 2003;11(3):139–149.
24. Chari RV. Targeted cancer therapy: conferring specificity to cytotoxic drugs. *Acc Chem Res*. 2008;41(1):98–107.
25. Murakami T, Tsuchida K, Hashida M, Imahori H. Size control of lipid-based drug carrier by drug loading. *Mol Biosyst*. 2010;6(5): 789–791.
26. Patil RR, Guhagarkar SA, Devarajan PV. Engineered nanocarriers of doxorubicin: a current update. *Crit Rev Ther Drug Carrier Syst*. 2008; 25(1):1–61.
27. Kataoka K, Matsumoto T, Yokoyama M, et al. Doxorubicin-loaded poly(ethylene glycol)-poly(beta-benzyl-l-aspartate) copolymer micelles: their pharmaceutical characteristics and biological significance. *J Control Release*. 2000;64(1–3):143–153.
28. Springate CM, Jackson JK, Gleave ME, Burt HM. Clusterin antisense complexed with chitosan for controlled intratumoral delivery. *Int J Pharm*. 2008;350(1–2):53–64.
29. Gupta AK, Gupta M. Synthesis and surface engineering of iron oxide nanoparticles for biomedical applications. *Biomaterials*. 2005;26(18): 3995–4021.
30. Choi HS, Liu W, Misra P, et al. Renal clearance of quantum dots. *Nat Biotechnol*. 2007;25(10):1165–1170.
31. Chouly C, Pouliquen D, Lucet I, Jeune JJ, Jallet P. Development of superparamagnetic nanoparticles for MRI: effect of particle size, charge and surface nature on biodistribution. *J Microencapsul*. 1996;13(3): 245–255.
32. Gref R, Minamitake Y, Peracchia MT, Trubetskoy V, Torchilin V, Langer R. Biodegradable long-circulating polymeric nanospheres. *Science*. 1994;263(5153):1600–1603.
33. Yoo HS, Lee KH, Oh JE, Park TG. In vitro and in vivo anti-tumor activities of nanoparticles based on doxorubicin-PLGA conjugates. *J Control Release*. 2000;68(3):419–431.

34. Stubbs M, McSheehy PM, Griffiths JR, Bashford CL. Causes and consequences of tumour acidity and implications for treatment. *Mol Med Today*. 2000;6(1):15–19.
35. Tannock IF, Rotin D. Acid pH in tumors and its potential for therapeutic exploitation. *Cancer Res*. 1989;49(16):4373–4384.
36. Wang H, Zhao Y, Wu Y, et al. Enhanced anti-tumor efficacy by co-delivery of doxorubicin and paclitaxel with amphiphilic methoxy PEG-PLGA copolymer nanoparticles. *Biomaterials*. 2011;32(32):8281–8290.
37. Desai MP, Labhasetwar V, Walter E, Levy RJ, Amidon GL. The mechanism of uptake of biodegradable microparticles in Caco-2 cells is size dependent. *Pharm Res*. 1997;14(11):1568–1573.
38. Panyam J, Labhasetwar V. Biodegradable nanoparticles for drug and gene delivery to cells and tissue. *Adv Drug Deliv Rev*. 2003;55(3):329–347.
39. Jordan A, Scholz R, Schnoy N, Wust P, Maier-Hauff K, Felix R. Differential endocytosis of magnetic fluid particles into human primary glioblastoma, neuronal and fibroblast cells in vitro. *Eur J Cell Biol*. 1997;(Suppl 47):32.
40. Weissleder R, Kelly K, Sun EY, Shtatland T, Josephson L. Cell-specific targeting of nanoparticles by multivalent attachment of small molecules. *Nat Biotechnol*. 2005;23(11):1418–1423.
41. Kohler N, Sun C, Wang J, Zhang M. Methotrexate-modified superparamagnetic nanoparticles and their intracellular uptake into human cancer cells. *Langmuir*. 2005;21(19):8858–8864.
42. Huang X, Teng X, Chen D, Tang F, He J. The effect of the shape of mesoporous silica nanoparticles on cellular uptake and cell function. *Biomaterials*. 2010;31(3):438–448.
43. Kohler N, Sun C, Fichtenholtz A, Gunn J, Fang C, Zhang M. Methotrexate-immobilized poly(ethylene glycol) magnetic nanoparticles for MR imaging and drug delivery. *Small*. 2006;2(6):785–792.
44. Chen B, Cheng J, Wu Y, et al. Reversal of multidrug resistance by magnetic $Fe_3O_4$ nanoparticle copolymerizating daunorubicin and 5-bromotetrandrine in xenograft nude-mice. *Int J Nanomedicine*. 2009;4:73–78.
45. Jiang Z, Chen BA, Xia GH, et al. The reversal effect of magnetic $Fe_3O_4$ nanoparticles loaded with cisplatin on SKOV3/DDP ovarian carcinoma cells. *Int J Nanomedicine*. 2009;4:107–114.
46. Widder KJ, Senyei AE, Ranney DF. In vitro release of biologically active Adriamycin by magnetically responsive albumin microspheres. *Cancer Res*. 1980;40(10):3512–3517.
47. Gupta PK, Hung CT. Magnetically controlled targeted chemotherapy. In: Willmott N, Daly J, editors. *Microspheres and Regional Cancer Therapy*. Boca Raton, FL: CRC Press; 1993:71–116.